NIH Public Access
Author Manuscript
Cell Signal. Author manuscript; available in PMC 2009 May 14.

Published in final edited form as:
Cell Signal. 2007 August ; 19(8): 1754–1764. doi:10.1016/j.cellsig.2007.03.011.

Pulmonary Endothelial Cell Barrier Enhancement by FTY720 Does Not Require the $S1P_1$ Receptor

SM Dudek, **SM Camp**, **ET Chiang**, **PA Singleton**, **PV Usatyuk**, **Y Zhao**, **Natarajan V**, and **JGN Garcia**
Section of Pulmonary & Critical Care Medicine, University of Chicago Pritzker School of Medicine, Chicago, Illinois

Abstract

Novel therapeutic strategies are needed to reverse the loss of endothelial cell (EC) barrier integrity that occurs during inflammatory disease states such as acute lung injury. We previously demonstrated potent EC barrier augmentation in vivo and in vitro by the platelet-derived phospholipid, sphingosine 1-phosphate (S1P) via ligation of the $S1P_1$ receptor. The S1P analogue, FTY720, similarly exerts barrier-protective vascular effects via presumed $S1P_1$ receptor ligation. We examined the role of the $S1P_1$ receptor in sphingolipid-mediated human lung EC barrier enhancement. Both S1P and FTY induced sustained, dose-dependent barrier enhancement, reflected by increases in transendothelial electrical resistance (TER), which was abolished by pertussis toxin indicating Gi-coupled receptor activation. FTY-mediated increases in TER exhibited significantly delayed onset and intensity relative to the S1P response. Reduction of $S1P_1$R expression (via siRNA) attenuated S1P-induced TER elevations whereas the TER response to FTY was unaffected. Both S1P and FTY rapidly (within 5 minutes) induced $S1P_1$R accumulation in membrane lipid rafts, but only S1P stimulated $S1P_1$R phosphorylation on threonine residues. Inhibition of PI3 kinase activity attenuated S1P-mediated TER increases but failed to alter FTY-induced TER elevation. Finally, S1P, but not FTY, induced significant myosin light chain phosphorylation and dramatic actin cytoskeletal rearrangement whereas reduced expression of the cytoskeletal effectors, Rac1 and cortactin (via siRNA), attenuated S1P-, but not FTY-induced TER elevations. These results mechanistically characterize pulmonary vascular barrier regulation by FTY720, suggesting a novel barrier-enhancing pathway for modulating vascular permeability.

Keywords

FTY720; sphingosine 1-phosphate; vascular permeability; Rac; cytoskeleton; G-coupled receptors

Introduction

Marked and sustained increased vascular permeability is an essential pathophysiological feature of acute inflammatory states such as acute lung injury (ALI) and sepsis and a major determinant of increased mortality. In the lung microcirculation, disruption of the pulmonary

Corresponding address: Steven M. Dudek, MD, Section of Pulmonary & Critical Care Medicine, Department of Medicine, University of Chicago, 5841 South Maryland Ave., Chicago, IL 60637, Phone: 773-834-2390, Fax: 773-702-6500, Email: E-mail: sdudek@medicine.bsd.uchicago.edu.

Publisher's Disclaimer: This is a PDF file of an unedited manuscript that has been accepted for publication. As a service to our customers we are providing this early version of the manuscript. The manuscript will undergo copyediting, typesetting, and review of the resulting proof before it is published in its final citable form. Please note that during the production process errors may be discovered which could affect the content, and all legal disclaimers that apply to the journal pertain.

NIH-PA Author Manuscript
NIH-PA Author Manuscript
NIH-PA Author Manuscript

NIH-PA Author Manuscript

NIH-PA Author Manuscript

NIH-PA Author Manuscript

vascular endothelial cell (EC) monolayer results in flooding of interstitial and alveolar compartments with fluid, protein, and inflammatory cells resulting in respiratory failure [1]. Unfortunately, specific therapies which prevent or reverse established vascular leak have been lacking. We recently described the potent EC barrier-enhancing properties of the platelet-derived sphingolipid, sphingosine 1-phosphate (S1P), which rapidly induces EC cytoskeletal rearrangements leading to augmented EC monolayer integrity [2]. Through ligation of the Gi-coupled $S1P_1$ receptor ($S1P_1R$), S1P initiates a series of downstream events, including Rac activation, cortactin translocation, peripheral myosin light chain (MLC) phosphorylation, and focal adhesion rearrangement, that result in enhancement of the EC cortical actin ring, improved cell-cell and cell-matrix interaction, and increased barrier function in vitro [2–4]. In addition, we have recently demonstrated the in vivo capacity for S1P to attenuate LPS-induced murine and canine models of sepsis and ALI [5,6], supporting the potential therapeutic utility of this compound in edema states.

FTY720 (2-amino-2-(2-[4-octylphenyl]ethyl)-1,3-propanediol), a synthesized derivative of the fungal compound, myriocin [7], has strong structural similarity to sphingosine and S1P and is currently in Phase III clinical trials as a immunosuppressive agent for the prevention of solid organ transplant rejection [8]. It has been reported that the mechanism of FTY-mediated immunosuppression involves binding to $S1P_1R$ on lymphocytes and internalizing the receptor, thereby inhibiting S1P-induced egress of lymphocytes from secondary lymphoid tissues and resulting in functional lymphopenia and impaired lymphocyte recirculation [9,10]. Because of the relatively low affinity of unphosphorylated FTY for the S1P receptor family [11], current concepts of FTY action invoke phosphorylation of FTY in situ (FTY-P) by cellular sphingosine kinases thereby greatly increasing the affinity for S1P family of receptors, particularly S1P1 and S1P3, eliciting downstream effects. This phosphorylation event occurs rapidly both in vitro and in vivo [12–14], although recent pharmacologic studies indicate that a substantial pool of circulating FTY (~25%) remains in the non-phosphorylated state in patients receiving FTY [12].

We and others have previously explored the capacity of FTY to modulate vascular permeability. FTY-P attenuated VEGF-induced mouse embryonic EC transmonolayer permeability in vitro, while oral FTY almost completely abolished vascular leak produced by VEGF injection in a murine ear assay [15]. More recently, we reported that a single intraperitoneal injection of FTY significantly attenuated multiple indices of murine pulmonary injury measured 24 hours after LPS administration [6]. While these provocative results suggest that FTY and related compounds may have clinical utility in the treatment of inflammatory syndromes, the exact mechanism of FTY action in preventing vascular leak remains unclear since FTY, unlike S1P, appears to internalize and downregulate $S1P_1R$ signaling instead of activating this pathway. A new paradigm has developed in which FTY appears to function as a $S1P_1R$ antagonist to exert its observed inhibitory effects on lymphocyte circulation [9,10, 16] and tumor angiogeneis [17]. These observations led us to rigorously explore the barrier regulatory properties of FTY in cultured human pulmonary EC. In this study we demonstrate that FTY potently enhances EC barrier function through a novel $S1P_1R$-independent mechanism that involves an alternative Gi-coupled receptor. These data advance our understanding of pulmonary vascular permeability and provide additional insight into barrier-regulatory pathways that may serve as useful clinical targets for modulation of vascular leak.

Experimental Materials and Methods

Reagents

Unless otherwise specified, reagents (including S1P) were obtained from Sigma (St. Louis, MO). KRN633 was purchased from Calbiochem (San Diego, CA). (R)-(+)-Methanandamide, arachidonyl-2′-chloroethylamide (ACEA), BML-190, AM 251, and AM 630 were obtained

NIH-PA Author Manuscript

NIH-PA Author Manuscript

NIH-PA Author Manuscript

from Tocris (Ellisville, MO). FTY720 was kindly provided by Novartis, while phosphorylated FTY720 (FTY-P) was kindly provided by Hugh Rosen (Scripps). Antibodies were obtained as follows: rabbit anti-diphosphorylated MLC, rabbit anti-pan MLC, rabbit anti-pan ERK, and rabbit anti-phospho-ERK (Cell Signaling, Beverly, MA), mouse anti-cortactin (Upstate Biotechnology, Lake Placid, NY), rabbit anti-pan AKT, and rabbit anti-phospho AKT sc-16646 (Santa Cruz Biotechnology, Santa Cruz, CA), rabbit anti-phosphothreonine (Zymed, South San Francisco, CA), rabbit anti-$S1P_1$ receptor (Affinity Bioreagents, Golden, CO) for Westerns, rabbit anti-$S1P_1$ receptor H-60 (Santa Cruz) for immunofluorescence, and mouse anti-$S1P_3$ receptor (Exalpha Biologicals, Watertown, MA). [^{32}P]-orthophosphate (carrier-free) was purchased from Perkin Elmer (Boston, MA).

Cell culture

Human pulmonary artery endothelial cells (HPAEC) obtained from Clonetics (Walkersville, MD) were cultured as previously described [4] in EBM-2 complete medium (Clonetics) at 37° C in a humidified atmosphere of 5%CO_2/95% air, with passages 6–10 used for experimentation. Wild type and $S1P_1R$ −/− mouse embryonic EC (MEEC), generous gifts from Drs. T. Hla and T. Sanchez (University of Connecticut), were isolated and cultured as previously described [18].

Adenoviral expression vectors and infection

SphK1-FLAG tagged adenoviral construct and sphK2-myc tagged adenoviral construct were constructed as follows. The SphK1 complete cDNA (GenBank™ accession number AF200328) with Flag tag, and the SphK2 complete cDNA (GenBank™ accession number BC010671) with c-myc tag were cloned into an adenoviral expression vector with cytomegalovirus promoter. The recombinant plasmids were linearized and propagated in HEK 293 cells, and the high-titer purified preparations (~10^{10} pfu/ml) were generated by the University of Iowa Gene Transfer Vector Core. HPAEC were infected at MOI=10 for 48 hours prior to experiments.

Transendothelial monolayer electrical resistance

EC were grown to confluence in polycarbonate wells containing evaporated gold microelectrodes, and TER measurements were then performed using an electrical cell-substrate impedance sensing system (ECIS) (Applied Biophysics, Troy, NY) as previously described in detail [2]. TER values from each microelectrode were pooled at discrete time points and plotted vs. time as the mean ± S.E.M.

Endothelial imaging

Human lung EC were grown on gelatinized cover slips before exposure to various conditions as described for individual experiments. EC were then fixed in 3.7% formaldehyde, permeabilized with 0.25% Triton X-100 for 5 minutes, washed in PBS, blocked with 2% BSA in PBS for 30 minutes, and then incubated for 60 minutes at room temperature with primary Ab of interest. After washing, EC were then incubated with appropriate secondary Ab conjugated to IF dyes (or Texas red-conjugated phalloidin for actin staining) for 60 minutes at room temperature. After further washing with PBS, cover slips were mounted using Slow Fade (Molecular Probes) and analyzed using a Nikon Eclipse TE 300 microscope and Sony Digital Photo camera DKC 5000. Images were recorded and saved in Adobe Photoshop.

MLC phosphorylation in intact endothelium

Human EC were analyzed for MLC phosphorylation by SDS-PAGE followed by Western immunoblotting with antibody specific for di-phosphorylated MLC (Cell Signaling). Multiple

NIH-PA Author Manuscript

NIH-PA Author Manuscript

NIH-PA Author Manuscript

blots were scanned and quantitatively analyzed using ImageQuant software (v5.2; Molecular Dynamics, Piscataway, NJ).

Construction and transfection of siRNA

The siRNA sequences targeting human cortactin, Rac1, $S1P_1R$, and $S1P_3R$ were generated using mRNA sequences from Gen-Bank™ (gi:20357555, 29792301, 13027635, and 38788192 respectively). To generate specific siRNA for these individual proteins, potential target (and scramble control) sequences were aligned to the human genome database in a BLAST search to eliminate sequences with significant homology to other human genes. For each mRNA (or scramble), two targets were identified. Specifically, the following sequences were used: cortactin (AATGCCTGGAAATTCCTCATT) (AAACAGAATTTCGTGAACAGC), Rac1 (AAAACTTGCCTACTGATCAGT) (AACTTGCCTACTGATCAGTTA), $S1P_1R$ (AAGCTACACAAAAAGCCTGGA) (AAAAA GCCTGGATCACTCATC), $S1P_3R$ (AACAGGGACTCAGGGACCAGA) (AAATGAATGTTCCTGGGGCGC), and scramble (AAGAGAAATCGAAACCGAAAA) (AAGAACCCAATTAAGCGCAAG). For construction of the siRNA, a transcription-based kit from Ambion (Austin, TX) was used (Silencer™ siRNA construction kit). EC cells were then transfected with siRNA using siPORTamine™ according to the manufacturer's protocol. Cells (~40% confluent) were serum-starved for 2 hours followed by incubation with 3 μM (1.5 μM of each siRNA) of target siRNA (or scramble siRNA) for 6 hours in serum-free media. Then media with serum was added (1% serum final concentration) for 42 hours before biochemical experiments and/or functional assays were conducted.

Determination of threonine phosphorylation of the $S1P_1$ receptor

EC monolayers were serum-starved for 2 hours followed by either vehicle, 1 μM S1P, or 1 μM FTY challenge for 5 min. Cells were subsequently solubilized in extraction buffer (50 mM HEPES (pH 7.5), 150 mM NaCl, 20 mM $MgCl_2$, 1% Triton X-100, 0.1% SDS, 0.4 mM Na_3VO_4, 40 mM NaF, 50 μM okadaic acid, 0.2 mM phenylmethylsulfonyl fluoride, 1:250 dilution of Calbiochem protease inhibitor mixture 3). The samples were then immunoprecipitated with rabbit anti-$S1P_1$ antibody followed by SDS-PAGE in 4–15% polyacrylamide gels and transfer onto Immobilon™ membranes (Millipore Corp., Bedford, MA). After blocking nonspecific sites with 5% BSA, the blots were incubated with rabbit anti-phosphothreonine antibody followed by incubating with horseradish peroxidase (HRP)-labeled goat anti-rabbit IgG. Visualization of immunoreactive bands was achieved using enhanced chemiluminescence (Amersham Biosciences).

Lipid raft isolation

Lipid rafts were isolated from human lung EC as previously described [19]. Briefly, EC were scraped in PBS, centrifuged at 2000 rpm at 4°C and lysed with 0.2 ml of TN solution [25 mM Tris–HCl (pH 7.5), 150 mM NaCl, 1 mM DTT, protease inhibitors, 10% sucrose, 1% Triton X-100] for 30 minutes on ice. Triton X-100-insoluble materials were then mixed with 0.6 ml of cold 60% Optiprep™ and overlaid with 0.6 ml of 40%, 35%, 30% and 20% Optiprep™ in TN solution. The gradients were centrifuged at 35,000 rpm in SW60 rotor for 12 hours at 4°C and different fractions were collected. Cellular proteins or lipids associated with each fraction were precipitated according to the procedures described previously and analyzed by SDS-PAGE plus immunoblotting and/or immunoprecipitation.

FTY phosphorylation assay

HPAECs (~70% confluence) were infected with adenoviral vector control or SphK1 wild type or SphK2 wild type (10 pfu/cell) for 48 hours and then were labeled with [^{32}P]-orthophosphate (20 μC_i/ml) in phosphate-free DMEM media for 3 hours. The media containing the

NIH-PA Author Manuscript

NIH-PA Author Manuscript

NIH-PA Author Manuscript

radioactivity was aspirated and cells were challenged with 1 ml of MEM medium alone or medium containing FTY or sphingosine (1 μM) in the presence of 0.1% BSA for 15 minutes. Lipid labeling was terminated by addition of 100 μl of 12N HCl followed by 2 ml of methanol. Cells were scraped, total extract was transferred to 15 ml glass tubes, lipids were partitioned into the chloroform phase by addition of 2 ml of chloroform and 700 μl of 1n HCl (to give a final ratio of 1:1:0.9 of chloroform:methanol:acidic aqueous phase), and vortexed. The lower chloroform phase containing the lipids was then dried under nitrogen, and the lipid extracts were subjected to thin layer chromatography on plastic Silica Gel 60 plates in the presence of cold S1P or FTYP as previously described [20,21].

Measurement of intracellular Ca^{2+}

HPAECs were plated on glass cover slips (Hitachi Instruments) and grown to ~95% confluence and intracellular Ca^{2+}concentration was monitored in basic media (mM): 116 NaCl, 5.37 KCl, 26.2 $NaHCO_3$, 1.8 $CaCl_2$, 0.81 $MgSO_4$, 1.02 $NaHPO_4$, 5.5 glucose, and 10 HEPES/HCl, pH 7.40, as previously described [22]. Briefly, cells were loaded with 5 μM Fura-2 AM for 15 minutes at 37°C in 5% CO_2-95% air in 1 ml of basic media in the presence of 0.1% BSA and 0.03% pluronic acid, rinsed twice and inserted diagonally in a 1.0 cm acrylic cuvette (Sarstedt, Newton, NC) filled with 3 ml incubation media at 37°C. Fura-2 fluorescence was measured with an Aminco-Bowman Series 2 luminescence spectrometer (SLM/Aminco, Urbana, IL) at excitation wavelengths of 340 and 380 nm and emission wavelength of 510 nm. Intracellular free calcium $[Ca^{2+}]_i$ in nM was calculated from the 340/380 ratio using software and calibration curves.

Immunoprecipitation and Western blotting

After treatment as outlined for individual experiments, EC were subsequently solubilized in extraction buffer (1% Triton X-100, 0.1% SDS, 50 mM HEPES (pH=7.5), 150 mM NaCl, 20 mM $MgCl_2$, 0.4 mM Na_3VO_4, 40 mM NaF, 50 nM okadaic acid, 0.2 mM phenylmethylsulfonyl fluoride, 1:250 dilution of Calbiochem protease inhibitor mixture 3). The samples were then immunoprecipitated with rabbit anti-$S1P_1$ antibody followed by SDS-PAGE in 4–15% gels and transfer onto Immobilon™ membranes (Millipore Corp., Bedford, MA). After blocking nonspecific sites with 5% BSA, the blots were incubated with either rabbit anti-$S1P_1$ antibody or rabbit anti-phosphothreonine antibody followed by incubation with HRP-labeled goat anti-rabbit IgG. Visualization of immunoreactive bands was achieved using enhanced chemiluminescence (Amersham Biosciences).

Statistical analysis

Student's *t*-test was used to compare the means of data from two or more different experimental groups. Results are expressed as means ± S.E.M.

Results

FTY720 enhances pulmonary endothelial cell barrier function

Our initial studies addressed the effect of FTY on human pulmonary EC barrier function as measured by transendothelial monolayer electrical resistance (TER), a highly sensitive measure of permeability. Similar to S1P [2], FTY produced dose-dependent and sustained increases in TER (indicative of enhanced EC barrier function) over a range of 0.01–10 μM, with a maximal effect observed at 1 μM (Fig. 1A). FTY-induced EC barrier enhancement occurred within a similar concentration range as S1P, despite a reported 500 fold decrease in FTY affinity [11] for the known barrier-promoting receptor $S1P_1R$ [2], and exhibited a delayed onset and slower rate of rise in TER relative to S1P. For example, FTY required 30–60 minutes

NIH-PA Author Manuscript

NIH-PA Author Manuscript

NIH-PA Author Manuscript

to achieve maximal barrier enhancement whereas comparable maximal TER levels were produced by S1P within 5 minutes (Fig. 1B).

We next hypothesized that this delay in maximal TER levels may be attributable to a requirement for FTY phosphorylation catalyzed by EC sphingosine kinases—a modification known to result in greatly increased affinity for $S1P_1R$, achieving affinities similar to S1P [11]—before binding these receptors and initiating barrier enhancement. However, the exogenous administration of previously phosphorylated FTY (FTY-P) only partially corrected this delayed rise in TER (Fig. 1B) despite similar binding affinity for $S1P_1R$ as S1P [11]. Thus, this delay in onset of FTY-mediated barrier enhancement, even when FTY-P is utilized, suggests the potential involvement of an alternative EC barrier-promoting pathway not utilizing $S1P_1R$.

FTY-induced EC barrier enhancement is independent of $S1P_1R$ ligation

To directly address whether $S1P_1R$ is involved in FTY-induced barrier enhancement, we generated a siRNA construct which selectively downregulates $S1P_1R$ protein expression by ~90% (see ref [23] for published Western blot confirmation). Consistent with our previously published data utilizing $S1P_1R$ antisense oligonucleotides [2], reduction in $S1P_1R$ expression via siRNA dramatically decreased S1P-induced EC barrier enhancement (Fig. 2A,B). Interestingly, we observed a delayed onset and slower rate of rise in TER after S1P challenge in $S1P_1R$ siRNA-treated EC, findings highly reminiscent of the response to FTY in normal EC monolayers (Fig. 1B). Reductions in $S1P_1R$ expression essentially did not affect FTY-induced TER elevation (Fig. 2B). Together, these data strongly support an alternative EC barrier-enhancing mechanism utilized by FTY which does not involve $S1P_1R$. EC also express relatively high levels of the $S1P_3$ receptor, but it does not appear to be responsible for FTY-induced barrier enhancement since siRNA depletion of this receptor did not affect FTY's TER effects (Fig. 2B).

Because of the remote possibility that residual $S1P_1R$ after our $S1P_1R$ siRNA therapy (less than 10% of the endogenous protein remained as quantified by Western blotting) was sufficient to allow for maximal FTY-, but not S1P-induced EC barrier enhancement, we also utilized embryonic EC isolated from $S1P_1R$ −/− mouse embryos for our TER experiments. $S1P_1R$ −/− mice exhibit embryonic hemorrhage leading to intrauterine death between E12.5 and E14.5 [24], however, embryonic EC can be isolated prior to this time and used for in vitro experimentation. Providing definitive evidence that $S1P_1R$ is not required for FTY-induced barrier enhancement, $S1P_1R$ −/− MEEC exhibited a robust 40% increase in TER following FTY stimulation (Fig. 2C). Interestingly, control MEEC isolated from $S1P_1R$ +/+ mice demonstrated only a modest 10% increase in TER after FTY (Fig. 2C). This finding may suggest compensatory upregulation of an as of yet unknown receptor in the $S1P_1R$ −/− MEEC that helps mediate FTY barrier enhancement. Studies are ongoing to identify this putative FTY receptor.

Characterization of differential EC intracellular signaling and cytoskeletal rearrangement in response to FTY compared to S1P

To further characterize the mechanistic differences between S1P- and FTY-induced barrier enhancement, we next explored their effects on calcium (Ca^{2+}) signaling. Previous studies have described a brief but substantial increase in intracellular Ca^{2+} following S1P exposure in multiple cell types [25]. We measured changes in HPAEC $[Ca^{2+}]_i$ after stimulation with 1 μM S1P, FTY, FTY-P, or vehicle (Fig. 3A–D). Only S1P produced a transient Ca^{2+} spike that was significantly different from the other conditions (Fig. 3E), demonstrating that FTY-induced EC barrier enhancement does not require the calcium signaling observed in association with S1P.

NIH-PA Author Manuscript

NIH-PA Author Manuscript

NIH-PA Author Manuscript

S1P generates EC cytoskeletal rearrangements that result in enhanced cortical actin accumulation and peripheral MLC phosphorylation, essential components in S1P-mediated pulmonary EC barrier enhancement [4]. Immunofluorescent staining (Fig. 4A) illustrates the characteristic cytoskeletal rearrangements evoked by S1P, as we have previously described [2]. In contrast, FTY failed to increase either cortical actin staining or peripheral MLC phosphorylation even after 30 minutes of exposure (Fig. 4A), a duration which FTY-induced EC barrier enhancement as measured by TER becomes maximal (Fig. 1). Similarly, neither FTY nor FTY-P increased levels of MLC phosphorylation in EC lysates while S1P produced substantial and sustained elevations in MLC phosphorylation (Fig. 4B). In addition, S1P rapidly activated ERK within 5 minutes whereas FTY and FTY-P failed to induce substantial ERK activation within this timeframe (Fig. 4B). Interestingly, S1P also induced a rearrangement in $S1P_1R$ immunofluorescence—from a predominantly peripheral linear pattern to more discrete clustering throughout the cell—that was not observed after FTY (Fig. 4A), providing further evidence that FTY does not enhance EC barrier function through the $S1P_1$ receptor.

To further characterize the mechanistic differences between S1P- and FTY-induced barrier enhancement, we generated siRNAs for both the small GTPase Rac1 and the actin-binding protein cortactin, cytoskeletal proteins we have previously demonstrated to be essential for optimal S1P barrier enhancement [4]. Downregulation of Rac1 or cortactin expression (~90% for each individual siRNA, data not shown), significantly attenuated the S1P-mediated TER elevation in a manner (magnitude, timecourse) similar to reduced $S1P_1R$ expression, but did not alter FTY-induced TER elevations (Fig. 4C). These data indicate that unlike S1P, FTY-induced EC barrier enhancement does not mechanistically require the $S1P_1R$-Rac1-cortactin transduction pathway necessary for S1P barrier promotion. Taken together, these data further support the hypothesis that S1P and FTY elicit distinct EC activation pathways, each of which results in barrier enhancement.

Phosphorylation of FTY is not required for EC barrier enhancement

Current concepts suggest that FTY requires phosphorylation by cellular sphingosine kinases for conversion into a high affinity S1PR ligand, before subsequent receptor binding and cellular activation. FTY serves as a substrate for both sphingosine kinase types 1 and 2 (SphK1 and SphK2) [13,14], a conversion which increases affinity for $S1P_1R$ by ~1500 fold [11]. We next sought to determine if FTY phosphorylation was necessary for FTY-induced EC barrier enhancement in vitro. To more definitively determine if FTY phosphorylation is a prerequisite to EC barrier enhancement, lipid extraction and 2-phase thin layer chromatography were utilized to directly measure [^{32}P]-orthophosphate incorporation into FTY in FTY–challenged EC pre-labeled with ^{32}P. Although incubation with sphingosine rapidly (within 5 minutes) resulted in formation of intracellular radiolabeled S1P (Fig. 5), radiolabeled phosphorylated FTY was not detected either intracellularly or in the extracellular media of FTY-challenged pulmonary EC over a 30 minutes incubation. Only after overexpression of SphK1 or SphK2 via adenoviral vector infection was FTY-P generation detected within the cells (Fig. 5). Moreover, overexpression of wild type SphK1 failed to augment maximal FTY-induced barrier enhancement (Fig. 6A), although the rate of rise in TER increased in a fashion similar to exogenously added FTY-P (data not shown). Together, these data strongly suggest that the phosphorylation of FTY is not essential for FTY-mediated increases in EC barrier integrity.

FTY-induced barrier enhancement is Gi-coupled and requires signaling through membrane lipid rafts

We next pursued a series of experiments designed to mechanistically explore alternative barrier-enhancing pathways through which FTY elicits barrier enhancement. Similar to S1P [2], preincubation with either pertussis toxin (PTX) or genestein, a nonspecific tyrosine kinase

NIH-PA Author Manuscript

NIH-PA Author Manuscript

NIH-PA Author Manuscript

inhibitor, significantly attenuated FTY-induced TER elevation (Fig. 6A), indicating involvement of a Gi-coupled receptor and tyrosine phosphorylation events in the FTY response. In contrast, VEGF receptor signaling does not appear to be involved in either S1P- or FTY-induced EC barrier enhancement since the VEGFR-1, -2, -3 inhibitor KRN633 failed to alter their TER responses (Fig. 6A) despite the known ability of S1P to transactivate the VEGF receptor in EC [26,27].

More recently, we have reported that signaling pathways initiated in membrane lipid rafts are essential to S1P-induced barrier enhancement [28]. The lipid raft disrupting agent, methyl-β-cyclodextrin (MβCD), also significantly attenuated FTY-induced TER, indicating that FTY requires these dynamic plasma membrane structures to exert its barrier promoting effects (Fig. 6A). Since both S1P and FTY require signaling through membrane lipid rafts, we next evaluated the composition of these structures and determined that whereas both S1P and FTY rapidly (within 5 minutes) recruit $S1P_1R$ and $S1P_3R$ to lipid raft fractions (Fig. 6B), only S1P induced the accumulation in the lipid raft fraction of activated (phosphorylated) Akt, a mechanism known to activate $S1P_1R$ signaling through phosphorylation of the $S1P_1R$ receptor [29]. Consistent with the divergent S1P and FTY receptor-mediated processes, immunoprecipitation of $S1P_1R$ from the lipid raft fraction after S1P challenge revealed substantial threonine phosphorylation of the $S1P_1R$ receptor (Fig. 6C), whereas FTY stimulated only delayed accumulation (at 30 minutes) of activated Akt in the lipid rafts without detectable phosphorylation of $S1P_1R$. Finally, inhibition of PI3 kinase activity (LY294002), which abolishes downstream activation of Akt, significantly attenuated S1P- but not FTY-induced TER elevations (Fig. 6A), providing further evidence that FTY-induced EC barrier enhancement evolves in a manner which is independent of $S1P_1R$ activation.

A recent report indicates that FTY also interacts with the CB_1 receptor of the cannabinoid family [30]. To explore whether this family of receptors is involved in FTY-induced EC barrier enhancement, we employed multiple cannabinoid agonists and antagonists to determine their effects on baseline and FTY-stimulated TER. Neither CB_1 (AM-251) nor CB_2 (AM-630) inhibitors blocked FTY-induced TER elevation, while the cannabinoid agonists (R)-(+)-Methanandamide, ACEA, and BML-190 all failed to augment baseline TER (Fig. 7). Thus, it seems unlikely that FTY mediates its EC barrier enhancing effects through CB_1 or CB_2 receptors.

Discussion

FTY serves as an effective novel immunomodulator in multiple models of transplant and autoimmune disease processes, such as renal graft rejection as well as animal models of autoimmune diabetes, encephalitis, and SLE [31–35]. In this study, we describe a novel pulmonary EC barrier enhancing pathway activated by FTY720 that is distinct from that utilized by the structurally-related sphingolipid, S1P. Several factors underscore the importance of generating detailed knowledge about FTY's mechanism of action. First, although S1P appears to be highly effective in reducing vascular leak in animal models of lung injury [5,6], the clinical utility of S1P is likely to be limited by well-described cardiovascular side effects mediated through ligation of $S1P_3R$ [25,36,37]. FTY has the obvious advantage of already being evaluated in advanced clinical trials which have demonstrated a favorable safety profile in renal transplant patients [12,35,38]. Although the safety of these compounds in critically ill patients with inflammatory lung syndromes or sepsis must still be determined, the recent development of multiple new structural analogues with various binding affinities for the S1PR family [36,37,39,40] facilitates this search for therapeutic agents for the treatment of inflammatory vascular leak. Secondly, the current paradigm holds that S1P mediates its barrier-promoting effects primarily through ligation of $S1P_1R$ [2]. Our siRNA data resulting in reduced $S1P_1R$ expression, however, suggest that the sustained portion of S1P-mediated EC

NIH-PA Author Manuscript

NIH-PA Author Manuscript

NIH-PA Author Manuscript

barrier enhancement may be, at least partially, $S1P_1R$ independent (Fig. 2). Therefore, understanding the mechanism(s) responsible for this prolonged enhancement of barrier integrity is of obvious clinical importance in the development of new therapeutic agents.

S1P ligation of $S1P_1R$ expressed on human pulmonary EC produces an almost immediate augmentation of barrier function that requires recruitment of $S1P_1R$ to membrane lipid rafts, Gi-coupled signaling, and Rac-dependent activation of downstream effectors PAK, LIM kinase, cofilin, and cortactin. These cytoskeletal effectors orchestrate a markedly increased cortical actin ring and rearrangement of focal adhesions (see summary diagram Fig. 8) [2–4, 28,41]. Although increased polymerized cortical actin is observed in association with multiple barrier-enhancing stimuli including S1P, shear stress, HGF, and simvastatin [2,42–44], FTY appears to be unique in its capacity to augment EC integrity without dramatic changes in cortical actin structure (Fig. 4A). Consistent with this observation, siRNA strategies to decrease expression of multiple proteins integral to generation of this cortical actin ring ($S1P_1R$, Rac, cortactin) each failed to alter FTY-induced TER elevation despite significant attenuation of S1P-induced barrier enhancement (Fig. 2, 4). Since these siRNA-driven strategies resulted in a delayed onset and slower rate of rise in TER after S1P in a manner analogous to FTY alone, the $S1P_1R$-Rac-cortactin-cortical actin pathway would appear to be responsible for the immediate barrier enhancement observed after S1P challenge, while an alternate, as yet poorly characrterized, mechanism is responsible for the sustained (over hours) augmentation of EC barrier integrity.

While admittedly little is known about this novel mechanism responsible for sustained EC barrier enhancement after FTY (Fig. 8), similar to S1P, this pathway requires intact membrane lipid rafts and is mediated through a Gi-coupled receptor as illustrated by MβCD and PTX inhibition of FTY-induced TER elevations (Fig. 6A). These data suggest an alternative G-protein coupled receptor (GPCR) may be involved in this process. Although FTY recruits $S1P_3R$ to lipid rafts (Fig. 6B), since siRNA-induced downregulation of $S1P_3R$ expression failed to alter FTY- (or S1P-) induced barrier enhancement (Fig. 2B), this receptor is unlikely to participate in the FTY barrier-regulatory response. The GPCR family is extensive and contains dozens of receptors with varying homologies to the S1PRs that could potentially participate in transducing FTY responses [45]. For example, a recent study describes involvement of a cardiac G-protein gated K^+ channel in FTY-induced bradycardia [46] in addition to the report of FTY interaction with the cannabinoid family of GPCRs discussed above [30]. Although our data suggest the primary cannabinoid receptors, CB_1 and CB_2, are not involved (Fig. 7), experiments are ongoing to determine the specific receptor responsible for FTY-induced barrier enhancement. Given that the nonspecific tyrosine kinase inhibitor genistein significantly attenuates FTY's effects (Fig. 6A), GPCRs known to couple to various receptor tyrosine kinases [47] will have particular interest. Additional insights into FTY's possible mechanism of action are provided by recent reports that it upregulates the EC junctional proteins PECAM, β-catenin, and ZO-1 [48] as well as promotes adherens junction assembly [15], suggesting that strengthening of cell-cell linkages may contribute to FTY-induced EC barrier enhancement (Fig. 8).

Earlier studies have emphasized that the majority of FTY is rapidly converted to FTY-P in vivo [12]. However, our data demonstrate that this phosphorylation event is not required for FTY-induced barrier enhancement, an observation contra to current concepts of FTY action. Although the SphK2 isoform is reportedly more effective at phosphorylating FTY in vitro [14], SphK1 is the predominantly expressed isoform both in EC and lung tissue [49]. However, upregulation of SphK1 activity with adenoviral overexpression failed to augment FTY-induced barrier enhancement (Fig. 6A). More importantly, using a highly sensitive 2-phase TLC assay, we failed to detect any significant incorporation of ^{32}P into FTY during the timeframe associated with FTY-induced TER elevation (Fig. 5). Despite modest FTY-P generation under

NIH-PA Author Manuscript

NIH-PA Author Manuscript

NIH-PA Author Manuscript

conditions of robust SphK1 or SphK2 overexpression, these data strongly indicate that conversion to FTY-P is not an essential prerequisite for FTY-mediated barrier promotion. Since non-phosphorylated FTY has relatively low affinity for the S1PR family, this observation provides further evidence that FTY promotes EC barrier integrity through a novel mechanistic pathway. It is interesting to note that exogenously administered FTY-P produced an earlier onset of TER elevation and a faster rate of rise than FTY, the timecourse of FTY-P barrier effects remained delayed relative to S1P, suggesting that the FTY-P species with its much higher affinity for $S1P_1R$ may enhance barrier function through the combined activation of both pathways (Fig. 8).

In summary, we have demonstrated potent and sustained EC barrier enhancement by FTY720 via a novel $S1P_1R$-independent mechanism. Although incompletely characterized, the barrier-enhancing pathway evoked by FTY should provide important insights into the mechanisms by which S1P and related compounds produce sustained reductions in vascular permeability which are observed for many hours after sphingolipid degradation. These data advance our understanding of pulmonary vascular permeability and important barrier-regulatory pathways that will hopefully serve to identify useful clinical targets for modulation of vascular leak during inflammatory syndromes.

Acknowledgements

This work was supported by grants from the National Heart Lung Blood Institute NIH grant P01 HL 58064 and R01 68071 (JGNG), RO1 HL 79396 (VN), and KO8 HL70013 (SMD). The wild type and $S1P_1R$ −/− mouse embryonic EC (MEEC) were generously provided by Drs. T. Hla and T. Sanchez (University of Connecticut). The authors gratefully acknowledge the contribution of Lakshmi Natarajan for her expert technical assistance.

References

1. Dudek SM, Garcia JGJ. Appl Physiol 2001;91(4):1487–1500.
2. Garcia JG, Liu F, Verin AD, Birukova A, Dechert MA, Gerthoffer WT, Bamberg JR, English D. J Clin Invest 2001;108(5):689–701. [PubMed: 11544274]
3. Shikata Y, Birukov KG, Garcia JG. J Appl Physiol 2003;94(3):1193–1203. [PubMed: 12482769]
4. Dudek SM, Jacobson JR, Chiang ET, Birukov KG, Wang P, Zhan X, Garcia JG. J Biol Chem 2004;279 (23):24692–24700. [PubMed: 15056655]
5. McVerry BJ, Peng X, Hassoun PM, Sammani S, Simon BA, Garcia JG. Am J Respir Crit Care Med 2004;170(9):987–993. [PubMed: 15282202]
6. Peng X, Hassoun PM, Sammani S, McVerry BJ, Burne MJ, Rabb H, Pearse D, Tuder RM, Garcia JG. Am J Respir Crit Care Med 2004;169(11):1245–1251. [PubMed: 15020292]
7. Im DS. Trends Pharmacol Sci 2003;24(1):2–4. [PubMed: 12498721]
8. Brinkmann V, Cyster JG, Hla T. Am J Transplant 2004;4(7):1019–1025. [PubMed: 15196057]
9. Matloubian M, Lo CG, Cinamon G, Lesneski MJ, Xu Y, Brinkmann V, Allende ML, Proia RL, Cyster JG. Nature 2004;427(6972):355–360. [PubMed: 14737169]
10. Graler MH, Goetzl EJ. Faseb J 2004;18(3):551–553. [PubMed: 14715694]
11. Mandala S, Hajdu R, Bergstrom J, Quackenbush E, Xie J, Milligan J, Thornton R, Shei GJ, Card D, Keohane C, Rosenbach M, Hale J, Lynch CL, Rupprecht K, Parsons W, Rosen H. Science 2002;296 (5566):346–349. [PubMed: 11923495]
12. Kovarik JM, Schmouder RL, Slade AJ. Ther Drug Monit 2004;26(6):585–587. [PubMed: 15570180]
13. Billich A, Bornancin F, Devay P, Mechtcheriakova D, Urtz N, Baumruker T. J Biol Chem 2003;278 (48):47408–47415. [PubMed: 13129923]
14. Paugh SW, Payne SG, Barbour SE, Milstien S, Spiegel S. FEBS Lett 2003;554(1–2):189–193. [PubMed: 14596938]
15. Sanchez T, Estrada-Hernandez T, Paik JH, Wu MT, Venkataraman K, Brinkmann V, Claffey K, Hla T. J Biol Chem 2003;278(47):47281–47290. [PubMed: 12954648]

NIH-PA Author Manuscript NIH-PA Author Manuscript NIH-PA Author Manuscript

16. Wei SH, Rosen H, Matheu MP, Sanna MG, Wang SK, Jo E, Wong CH, Parker I, Cahalan MD. Nat Immunol 2005;6(12):1228–1235. [PubMed: 16273098]
17. LaMontagne K, Littlewood-Evans A, Schnell C, O'Reilly T, Wyder L, Sanchez T, Probst B, Butler J, Wood A, Liau G, Billy E, Theuer A, Hla T, Wood J. Cancer Res 2006;66(1):221–231. [PubMed: 16397235]
18. Kluk MJ, Colmont C, Wu MT, Hla T. FEBS Lett 2003;533(1–3):25–28. [PubMed: 12505153]
19. Bourguignon LY, Singleton PA, Diedrich F, Stern R, Gilad E. J Biol Chem 2004;279(26):26991–27007. [PubMed: 15090545]
20. Berdyshev EV, Gorshkova IA, Usatyuk PV, Zhao Y, Saatian B, Hubbard W, Natarajan V. Cellular Signaling. 2006in press
21. Martin A, Duffy PA, Liossis C, Gomez-Munoz A, O'Brien L, Stone JC, Brindley DN. Oncogene 1997;14(13):1571–1580. [PubMed: 9129148]
22. Usatyuk PV, Fomin VP, Shi S, Garcia JG, Schaphorst K, Natarajan V. Am J Physiol Lung Cell Mol Physiol 2003;285(5):L1006–1017. [PubMed: 12882766]
23. Finigan JH, Dudek SM, Singleton PA, Chiang ET, Jacobson JR, Camp SM, Ye SQ, Garcia JG. J Biol Chem 2005;280(17):17286–17293. [PubMed: 15710622]
24. Liu Y, Wada R, Yamashita T, Mi Y, Deng CX, Hobson JP, Rosenfeldt HM, Nava VE, Chae SS, Lee MJ, Liu CH, Hla T, Spiegel S, Proia RL. J Clin Invest 2000;106(8):951–961. [PubMed: 11032855]
25. Sanna MG, Liao J, Jo E, Alfonso C, Ahn MY, Peterson MS, Webb B, Lefebvre S, Chun J, Gray N, Rosen H. J Biol Chem 2004;279(14):13839–13848. [PubMed: 14732717]
26. Endo A, Nagashima K, Kurose H, Mochizuki S, Matsuda M, Mochizuki N. J Biol Chem 2002;277(26):23747–23754. [PubMed: 11956190]
27. Tanimoto T, Jin ZG, Berk BC. J Biol Chem 2002;277(45):42997–43001. [PubMed: 12226078]
28. Singleton PA, Dudek SM, Chiang ET, Garcia JG. Faseb J 2005;19(12):1646–1656. [PubMed: 16195373]
29. Lee MJ, Thangada S, Paik JH, Sapkota GP, Ancellin N, Chae SS, Wu M, Morales-Ruiz M, Sessa WC, Alessi DR, Hla T. Mol Cell 2001;8(3):693–704. [PubMed: 11583630]
30. Paugh SW, Cassidy MP, He H, Milstien S, Sim-Selley LJ, Spiegel S, Selley DE. Mol Pharmacol 2006;70(1):41–50. [PubMed: 16571654]
31. Rausch M, Hiestand P, Foster CA, Baumann DR, Cannet C, Rudin M. J Magn Reson Imaging 2004;20(1):16–24. [PubMed: 15221804]
32. Okazaki H, Hirata D, Kamimura T, Sato H, Iwamoto M, Yoshio T, Masuyama J, Fujimura A, Kobayashi E, Kano S, Minota S. J Rheumatol 2002;29(4):707–716. [PubMed: 11950011]
33. Maki T, Gottschalk R, Monaco AP. Transplantation 2002;74(12):1684–1686. [PubMed: 12499880]
34. Webb M, Tham CS, Lin FF, Lariosa-Willingham K, Yu N, Hale J, Mandala S, Chun J, Rao TS. J Neuroimmunol 2004;153(1–2):108–121. [PubMed: 15265669]
35. Tedesco-Silva H, Mourad G, Kahan BD, Boira JG, Weimar W, Mulgaonkar S, Nashan B, Madsen S, Charpentier B, Pellet P, Vanrenterghem Y. Transplantation 2004;77(12):1826–1833. [PubMed: 15223899]
36. Hale JJ, Doherty G, Toth L, Mills SG, Hajdu R, Keohane CA, Rosenbach M, Milligan J, Shei GJ, Chrebet G, Bergstrom J, Card D, Forrest M, Sun SY, West S, Xie H, Nomura N, Rosen H, Mandala S. Bioorg Med Chem Lett 2004;14(13):3501–3505. [PubMed: 15177461]
37. Forrest M, Sun SY, Hajdu R, Bergstrom J, Card D, Doherty G, Hale J, Keohane C, Meyers C, Milligan J, Mills S, Nomura N, Rosen H, Rosenbach M, Shei GJ, Singer II, Tian M, West S, White V, Xie J, Proia RL, Mandala S. J Pharmacol Exp Ther 2004;309(2):758–768. [PubMed: 14747617]
38. Kahan BD, Karlix JL, Ferguson RM, Leichtman AB, Mulgaonkar S, Gonwa TA, Skerjanec A, Schmouder RL, Chodoff L. Transplantation 2003;76(7):1079–1084. [PubMed: 14557756]
39. Hale JJ, Yan L, Neway WE, Hajdu R, Bergstrom JD, Milligan JA, Shei GJ, Chrebet GL, Thornton RA, Card D, Rosenbach M, HughRosen, Mandala S. Bioorg Med Chem 2004;12(18):4803–4807. [PubMed: 15336258]
40. Hale JJ, Neway W, Mills SG, Hajdu R, Ann Keohane C, Rosenbach M, Milligan J, Shei GJ, Chrebet G, Bergstrom J, Card D, Koo GC, Koprak SL, Jackson JJ, Rosen H, Mandala S. Bioorg Med Chem Lett 2004;14(12):3351–3355. [PubMed: 15149705]

NIH-PA Author Manuscript

NIH-PA Author Manuscript

NIH-PA Author Manuscript

41. Shikata Y, Birukov KG, Birukova AA, Verin A, Garcia JG. Faseb J 2003;17(15):2240–2249. [PubMed: 14656986]

42. Liu F, Schaphorst KL, Verin AD, Jacobs K, Birukova A, Day RM, Bogatcheva N, Bottaro DP, Garcia JG. Faseb J 2002;16(9):950–962. [PubMed: 12087056]

43. Jacobson JR, Dudek SM, Birukov KG, Ye SQ, Grigoryev DN, Girgis RE, Garcia JG. Am J Respir Cell Mol Biol 2004;30(5):662–670. [PubMed: 14630613]

44. Birukov KG, Birukova AA, Dudek SM, Verin AD, Crow MT, Zhan X, DePaola N, Garcia JG. Am J Respir Cell Mol Biol 2002;26(4):453–464. [PubMed: 11919082]

45. Im DS. J Lipid Res 2004;45(3):410–418. [PubMed: 14657204]

46. Koyrakh L, Roman MI, Brinkmann V, Wickman K. Am J Transplant 2005;5(3):529–536. [PubMed: 15707407]

47. Pyne NJ, Waters C, Moughal NA, Sambi BS, Pyne S. Biochem Soc Trans 2003;31(Pt 6):1220–1225. [PubMed: 14641030]

48. Singer II, Tian M, Wickham LA, Lin J, Matheravidathu SS, Forrest MJ, Mandala S, Quackenbush EJ. J Immunol 2005;175(11):7151–7161. [PubMed: 16301618]

49. Ancellin N, Colmont C, Su J, Li Q, Mittereder N, Chae SS, Stefansson S, Liau G, Hla T. J Biol Chem 2002;277(8):6667–6675. [PubMed: 11741921]

NIH-PA Author Manuscript
NIH-PA Author Manuscript
NIH-PA Author Manuscript

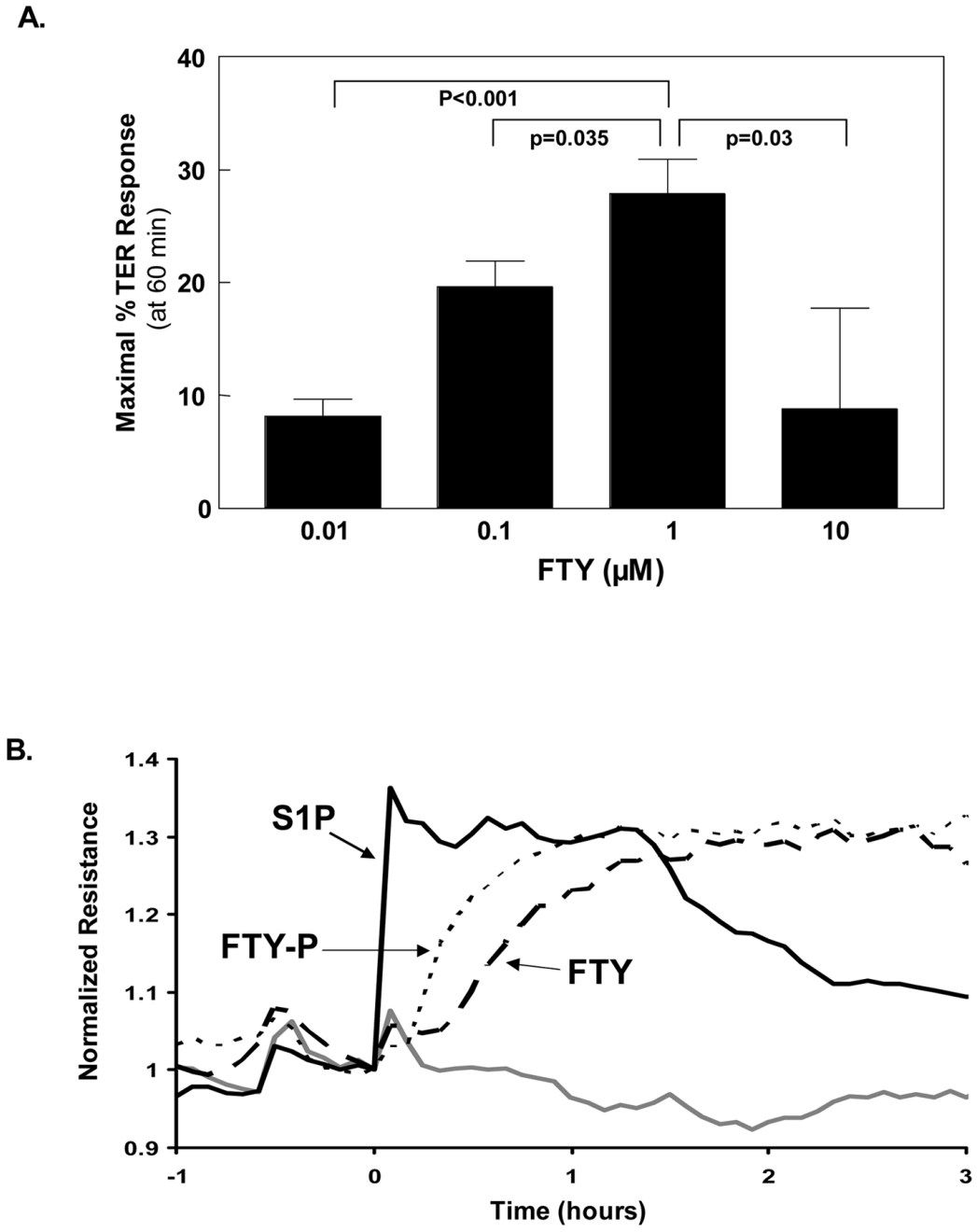

Figure 1. FTY720 enhances pulmonary EC barrier function in a dose-dependent but delayed manner relative to S1P

A) Concentration-dependent EC barrier enhancement by FTY. Human pulmonary artery endothelial cells (HPAEC) were plated in monolayer on gold microelectrodes and grown to confluence to measure transendothelial electrical resistance (TER) as described in Methods. The bar graph depicts TER data (+/− S.E.M.) as maximal % TER elevation induced with 60 min by FTY at concentrations from 0.01–10 μM vs. untreated controls. n=6–10 independent experiments per condition. **B) Differential rate of barrier enhancement by various sphingolipids.** Representative TER tracings for EC barrier enhancement at equivalent

concentrations (1 μM) of S1P (—), FTY (---), or FTY-P (···) are shown. The gray line represents vehicle-stimulated control EC. Experiments were independently performed at least 5 times.

NIH-PA Author Manuscript
NIH-PA Author Manuscript
NIH-PA Author Manuscript

NIH-PA Author Manuscript
NIH-PA Author Manuscript
NIH-PA Author Manuscript

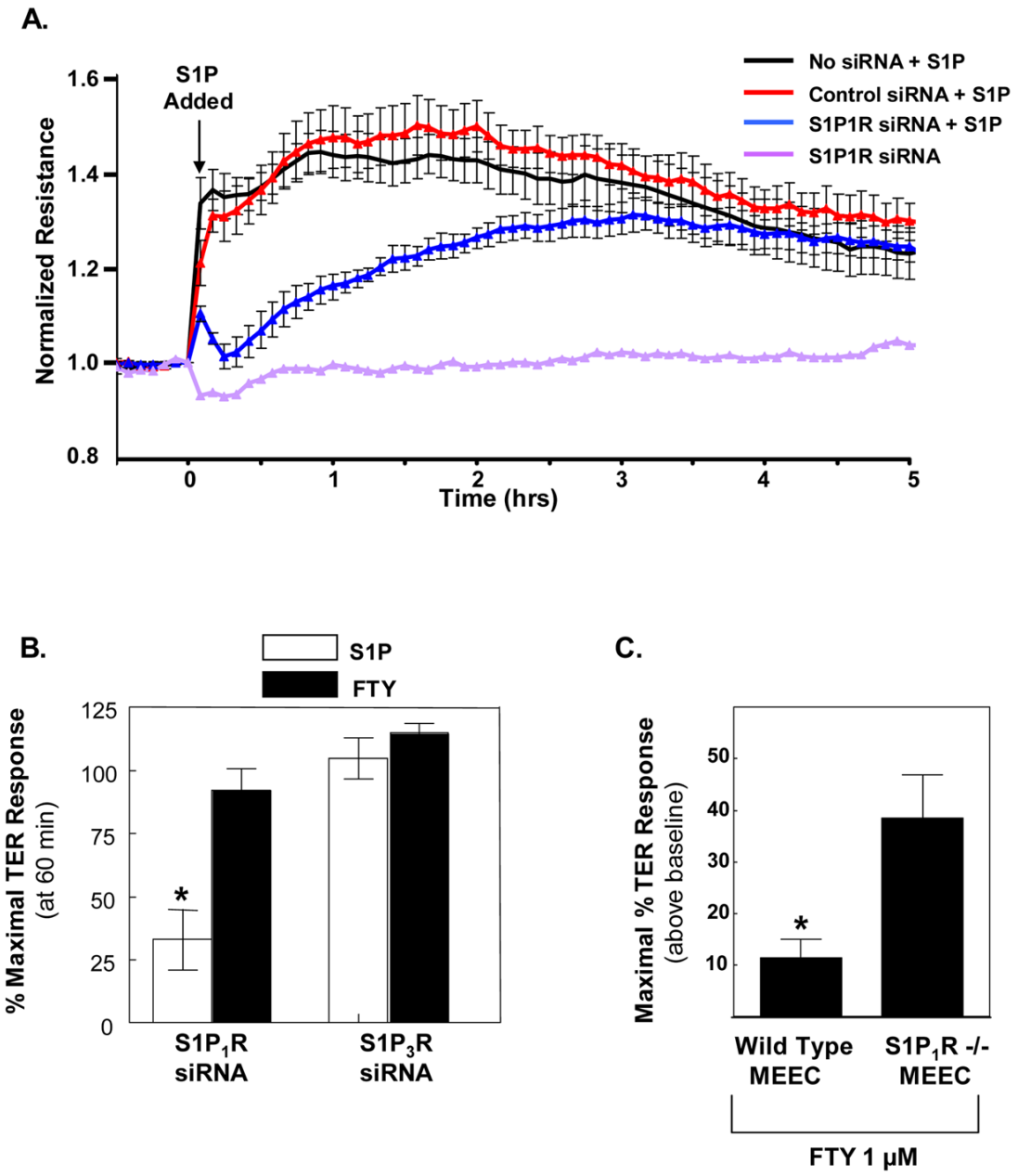

Figure 2. FTY-induced barrier enhancement is not dependent on $S1P_1R$

A) HPAEC plated on gold microelectrodes were transfected with $S1P_1R$ siRNA, scrambled control siRNA, or mock control transfection (as described in Methods) and then stimulated with S1P (1 μM) at time=0 (arrow). The TER tracing represents pooled data (+ S.E.M.) from 4 independent experiments. **B)** The bar graph depicts pooled TER data from HPAEC transfected with $S1P_1R$ siRNA or $S1P_3R$ siRNA and then stimulated with 1 μM S1P (white bars) or 1 μM FTY (black bars). The data are expressed as percent maximal barrier enhancement (+/− S.E.M.) obtained within 60 min in scramble control siRNA transfected EC. n=3–5 independent experiments per condition. *p<0.01 vs. all other conditions. **C)** Wild type or $S1P_1R$ −/− mouse embryonic EC were plated on gold microelectrodes as per Methods and

NIH-PA Author Manuscript

NIH-PA Author Manuscript

NIH-PA Author Manuscript

then stimulated with FTY 1 μM. The data represent maximal increased TER (+/− S.E.M.) above baseline observed following stimulation (n=4 per condition). *p=0.01.

NIH-PA Author Manuscript

NIH-PA Author Manuscript

NIH-PA Author Manuscript

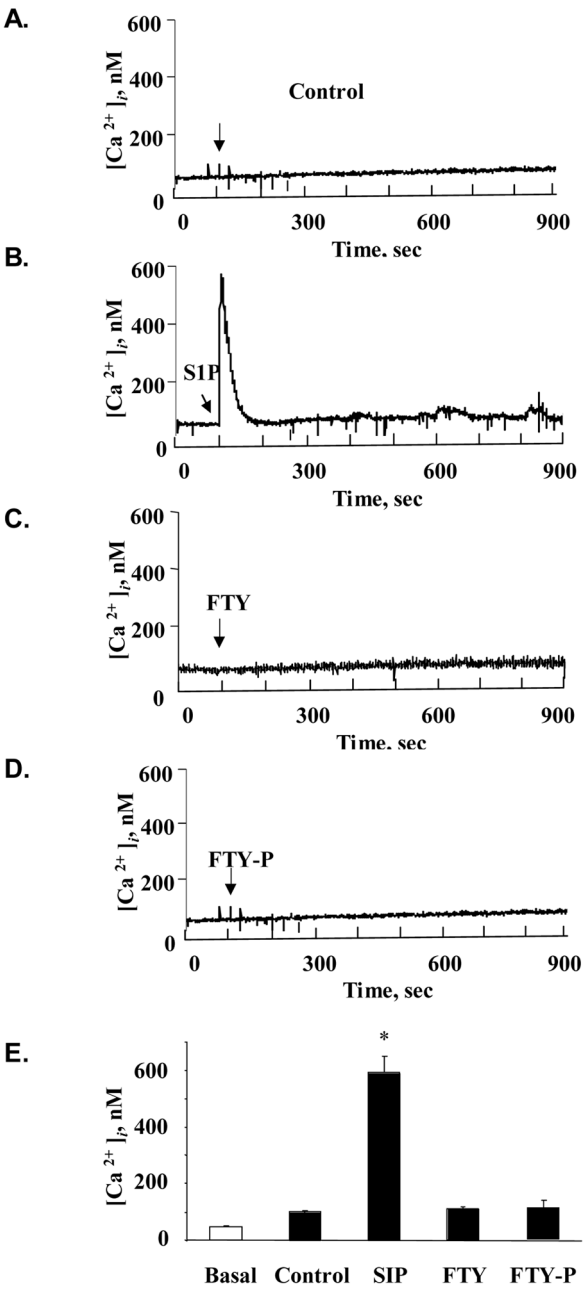

Figure 3. FTY does not stimulate intracellular calcium release

Cultured HPAEC intracellular calcium concentrations were measured as described in Methods following stimulation with vehicle (**A**), S1P 1 μM (**B**), FTY 1 μM (**C**), or FTY-P 1 μM (**D**). Rapid but transient increase was detected following S1P but not the other conditions. **E)** The bar graph depicts pooled maximal intracellular calcium detected following stimulation (n=3 per condition). *p<0.05 vs. all other conditions.

NIH-PA Author Manuscript

NIH-PA Author Manuscript

NIH-PA Author Manuscript

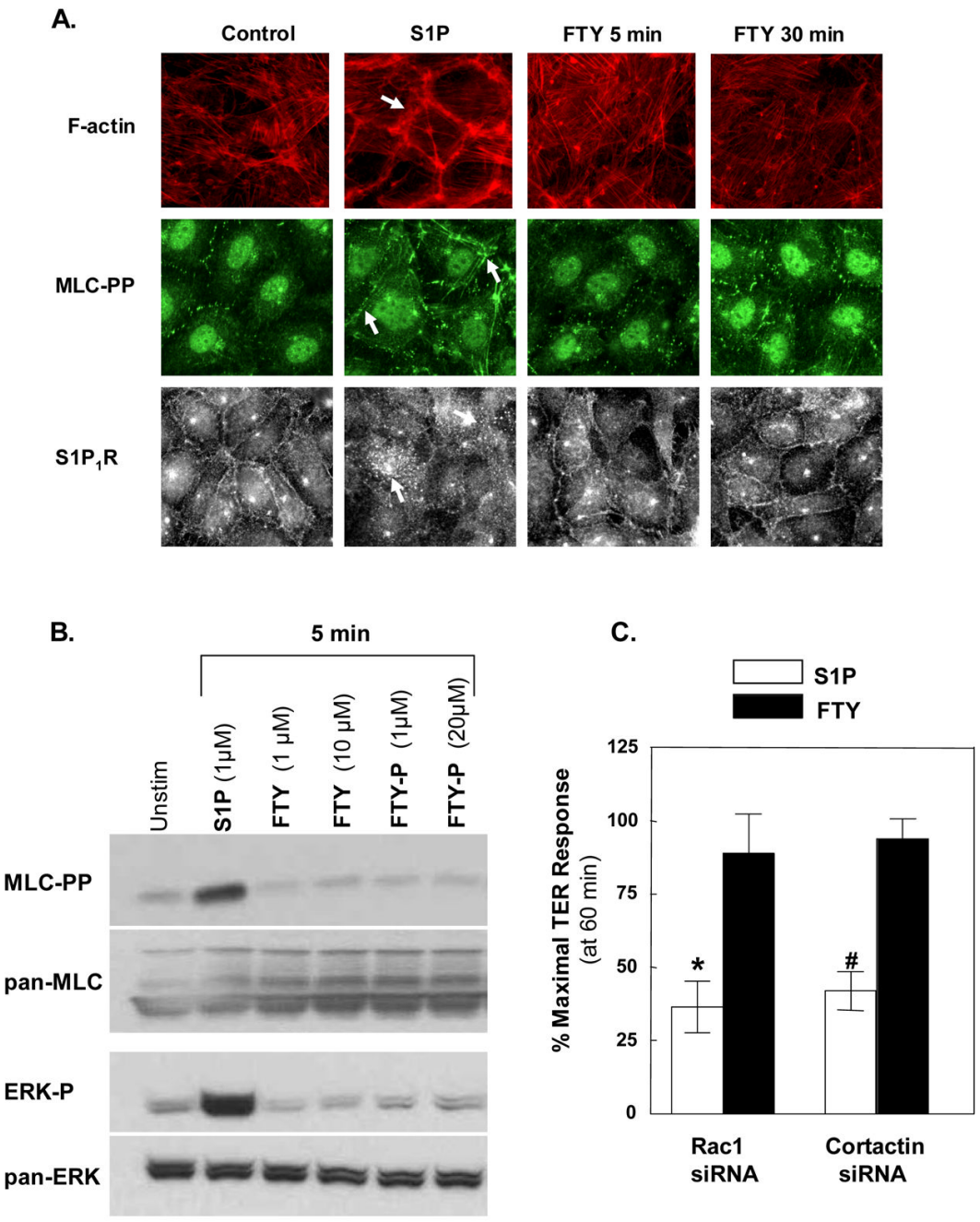

Figure 4. FTY-induced barrier enhancement does not involve dramatic cytoskeletal rearrangement as seen with S1P

A) Confluent HPAEC were stimulated with S1P 1μM for 5 min or FTY 1μM for 5 or 30 min. Cells were then fixed using formaldehyde and stained with phalloidin for F-actin (red), diphosphorylated myosin light chain (MLC-pp) antibody (green), or $S1P_1R$ antibody (gray scale). Arrows indicate increased cortical actin, increased peripheral ppMLC, and loss of peripheral $S1P_1R$ in S1P-stimulated EC. **B)** Confluent HPAEC were stimulated with S1P, FTY, or FTY-P (concentrations as above) for 0–5 min and then lysed for Western blotting. Note that all wells represent equal loading of total proteins. Experiments were performed in triplicate with reproducible findings (representative data shown). **C)** The bar graph depicts pooled TER

NIH-PA Author Manuscript

NIH-PA Author Manuscript

NIH-PA Author Manuscript

data from HPAEC transfected with Rac1 siRNA or cortactin siRNA and then stimulated with 1 μM S1P (white bars) or FTY (black bars). The data are expressed as percent maximal barrier enhancement at 60 min relative to control siRNA transfected EC. n=6–8 independent experiments per condition. *$p<0.005$ vs. FTY-stimulated Rac1 siRNA-treated EC. #$p<0.001$ vs. FTY-stimulated cortactin siRNA-treated EC. Note that FTY-stimulated Rac1 or cortactin siRNA-treated EC are not statistically different from FTY-stimulated control siRNA transfected EC.

NIH-PA Author Manuscript

NIH-PA Author Manuscript

NIH-PA Author Manuscript

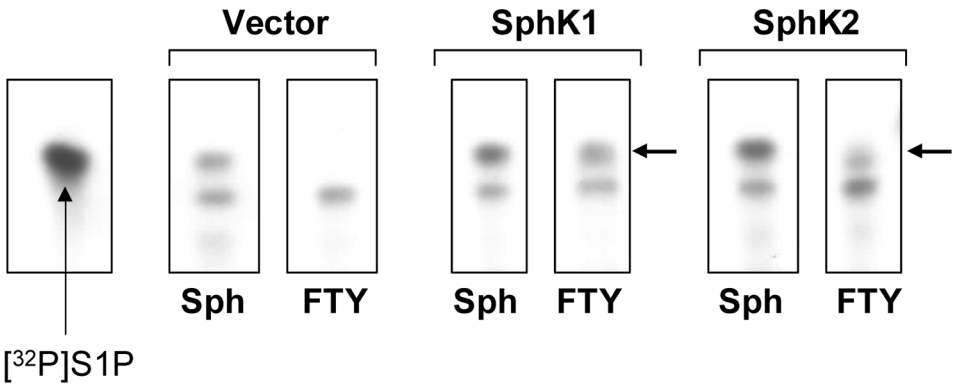

Figure 5. Phosphorylation status of FTY in EC

Adenoviral overexpression of HPAEC (MOI=10) with vector, sphingosine kinase 1 (SphK1), or sphingosine kinase 2 (SphK2) was performed as per Methods. EC were then labeled with ^{32}P for several hours before incubation with precursors sphingosine (Sph) or FTY for 15 min. Lipid extraction was performed and then subjected to 2-phase thin layer chromatography. Radiolabeled exogenous S1P was run in the first lane as a marker control. In vector infected EC, Sph is phosphorylated to S1P, but no FTY-P is detected after FTY addition. However, in both SphK1 and SphK2 overexpressing EC, FTY conversion to FTY-P is seen (black arrows).

NIH-PA Author Manuscript

NIH-PA Author Manuscript

NIH-PA Author Manuscript

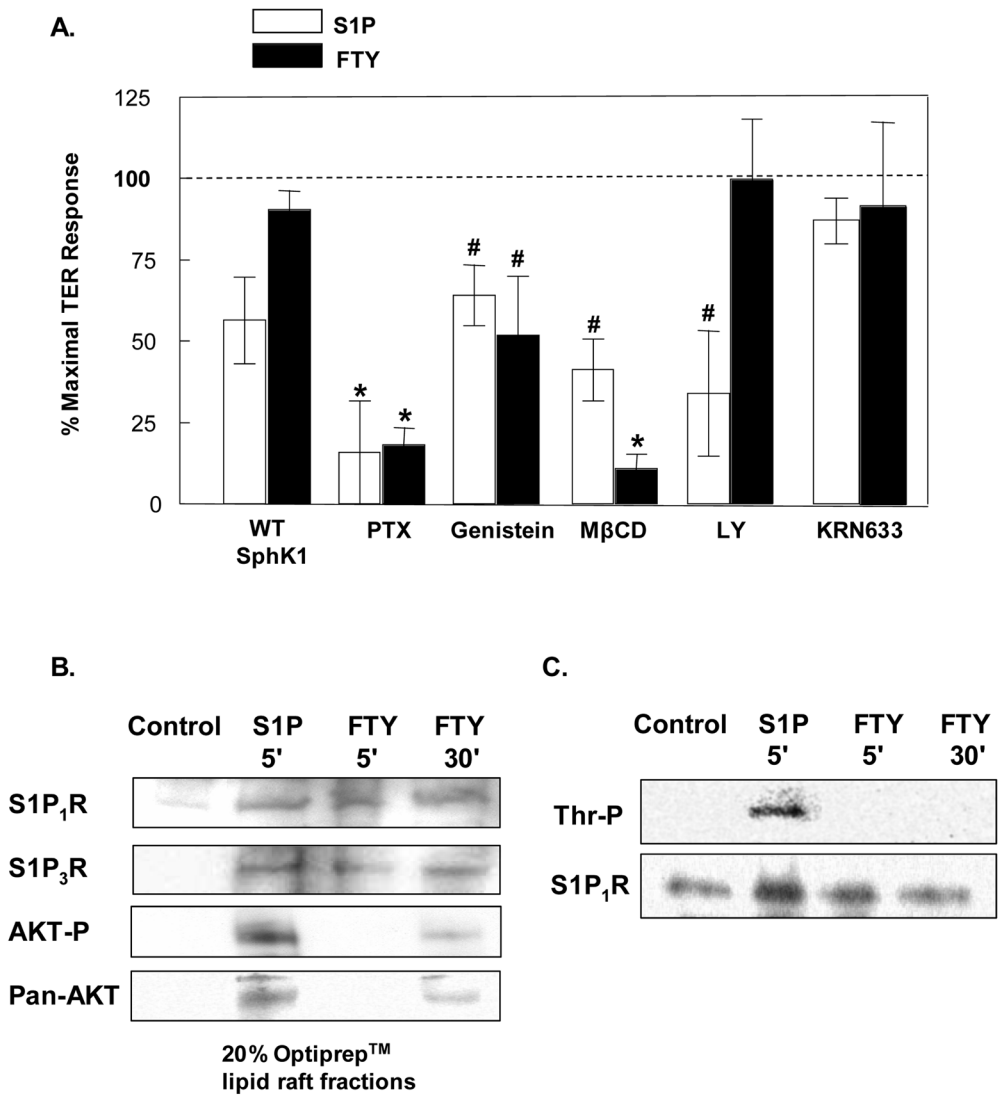

Figure 6. FTY-induced barrier enhancement is Gi-coupled and requires signaling through membrane lipid rafts but does not phosphorylate $S1P_1R$

A) Confluent HPAEC were stimulated with 1 μM S1P (white bars) or FTY (black bars) 48 hrs after infection with wild type SphK1 adenovirus (MOI=10), or after a 2 hour preincubation with 100 ng/ml Pertussis toxin (PTX), 30 min preincubation with 200 μM Genistein, one hr preincubations with 10 mM methyl-β-cyclodextrin (MβCD), LY294002 (10 μM), or KRN633 (100 nM). The data are expressed as percent maximal barrier enhancement at 60 min relative to control viral-infected or vehicle-treated EC. n=3–10 independent experiments per condition. *p<0.001 vs. S1P or FTY-stimulated, control EC. #p<0.05 vs. S1P or FTY-stimulated, control EC. **B)** Confluent HPAEC were stimulated with either vehicle (control), 1 μM S1P (5 min), or 1 μM FTY (5 or 30 min) and then solubilized in 4°C Triton X-100 and treated with Optiprep™ as described in Methods to isolate lipid rafts. Immunoblot anaylsis of the 20% Optiprep™ lipid raft- containing fractions was performed using anti-$S1P_1R$, anti-$S1P_3R$, anti-AKT-P, and anti- Pan-AKT antibodies. Experiments were performed in triplicate each with similar results. Representative data are shown. **C)** Confluent HPAEC were stimulated with either vehicle (control), 1 μM S1P (5 min), or 1 μM FTY (5 or 30 min). $S1P_1R$ was then immunoprecipitated from the EC lysates (as described in Methods) and probed with

phosphothreonine antibody to determine phosphorylation status of the receptor. Experiments were performed in triplicate each with similar results. Representative data are shown.

NIH-PA Author Manuscript
NIH-PA Author Manuscript
NIH-PA Author Manuscript

NIH-PA Author Manuscript

NIH-PA Author Manuscript

NIH-PA Author Manuscript

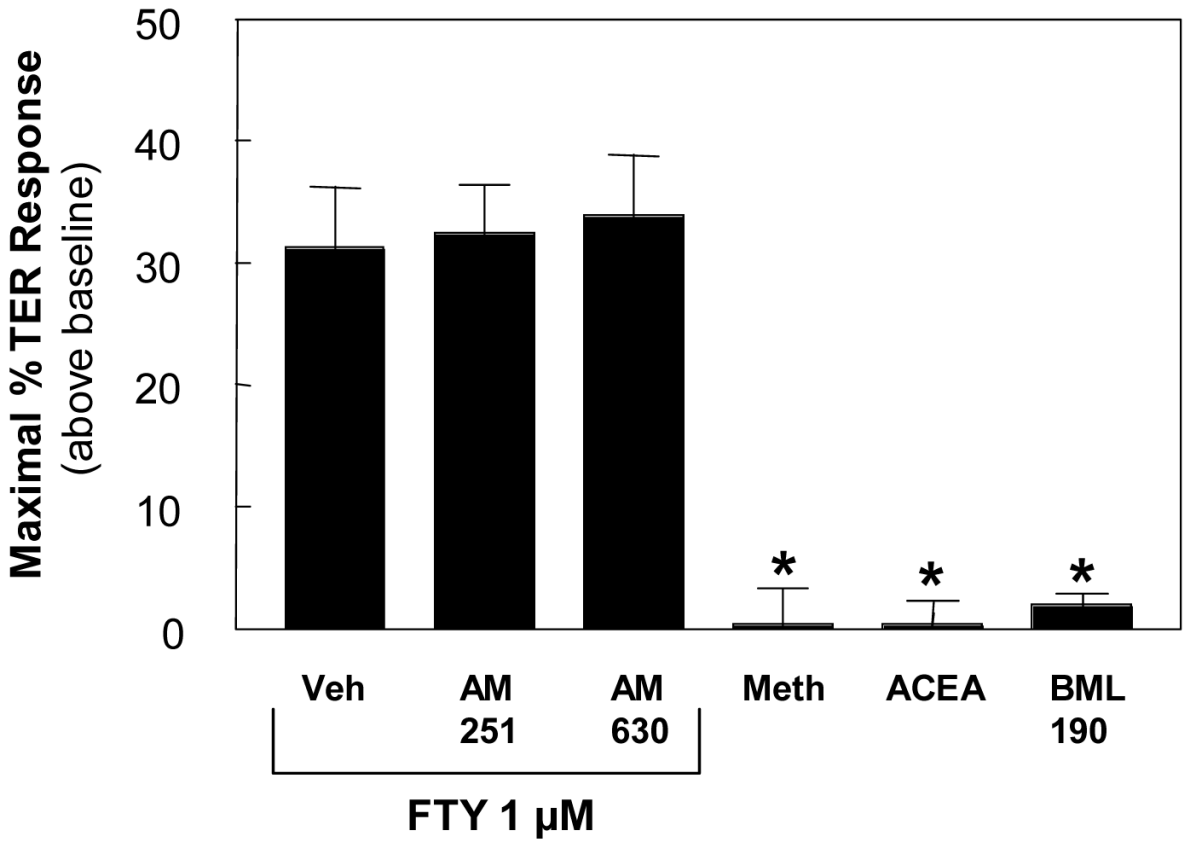

Figure 7. The Cannabinoid receptors do not mediate FTY-induced EC barrier enhancement

HPAEC were plated on gold microelectrodes as per Methods and then stimulated with FTY (1 μM) plus CB_1 antagonist AM-251 (0.5 μM), CB_2 antagonist AM-630 (0.5 μM), or vehicle. In parallel experiments, EC were directly stimulated by the general cannabinoid receptor agonist (R)-(+)-Methanandamide (1 μM), the CB_1 agonist ACEA (0.5 μM), or the CB_2 agonist BML-190 (5 μM). The data represent maximal increased TER (+/− S.E.M.) above baseline observed following stimulation (n=4–6 per condition). *p<0.001 vs. FTY alone (Vehicle).

NIH-PA Author Manuscript

NIH-PA Author Manuscript

NIH-PA Author Manuscript

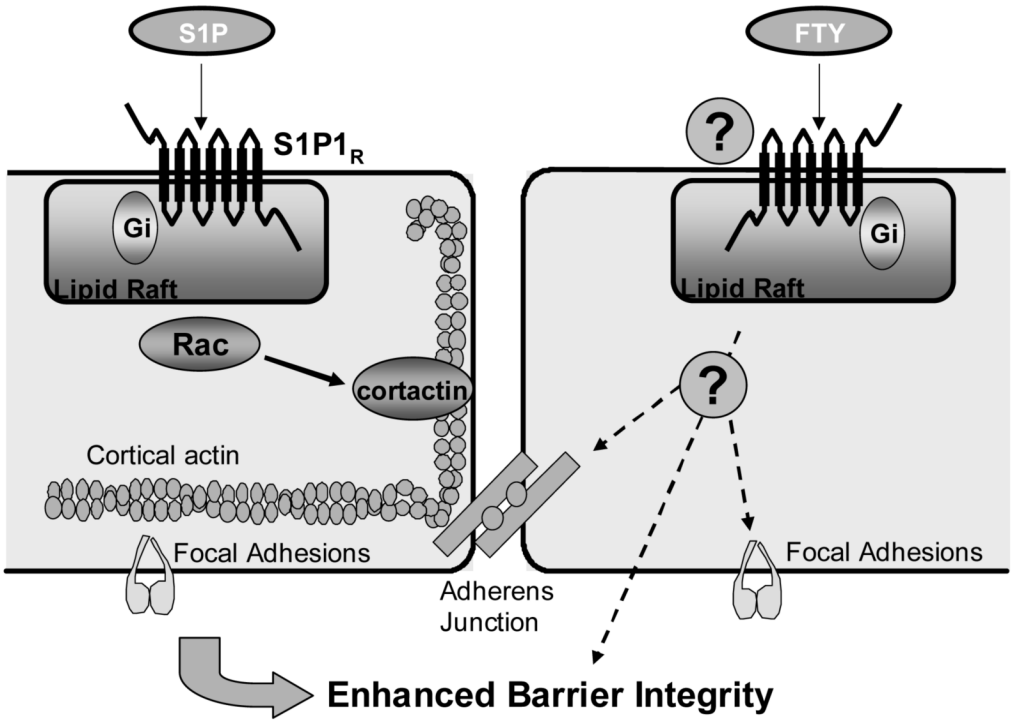

Figure 8. Summary diagram outlining differential signaling pathways involved in FTY and S1P-induced EC barrier enhancement

Depicted on the left is a schematic representation of the major components involved in mediating S1P-induced endothelial cell barrier enhancement. Extracellular S1P ligates the Gi-coupled $S1P_1$ receptor with subsequent Rac-dependent activation of multiple downstream effectors including cortactin, resulting in markedly increased cortical actin ring and rearrangement of focal adhesions [2–4,28,41]. On the right, FTY-induced EC barrier enhancement requires intact membrane lipid rafts and is mediated through a Gi-coupled receptor, but in contrast to S1P, Rac-dependent effects such as cortactin translocation and cortical actin ring formation are not essential components. The downstream mechanisms responsible for FTY-induced EC barrier enhancement are still unclear, but the authors hypothesize that enhanced cell-cell (represented by cadherin-linked adherens junctions) [15] and cell-matrix (integrin-linked focal adhesions) may be involved.